



NIWA

Taihoru Nukurangi

**Estimation of acoustic target strength of hoki
using *in situ* data and swimbladder modelling**

P. Cordue, G. Macaulay, P. Grimes

**Final Research Report for
Ministry of Fisheries Research Project HOK9803
Objective 2**

National Institute of Water and Atmospheric Research

August 2000

Final Research Report

Report Title	Estimation of acoustic target strength of hoki using <i>in situ</i> data and swimbladder modelling
Authors	Patrick Cordue, Gavin Macaulay and Paul Grimes
1. Date:	31 May 2000
2. Contractor:	National Institute of Water and Atmospheric Research Limited
3. Project Title:	Estimation of spawning hoki biomass using acoustic surveys
4. Project Code:	HOK9803
5. Project Leader:	Patrick Cordue
6. Duration of Project:	
Start date:	1 October 1998
Completion date:	31 May 2000

7. Executive Summary

Acoustic target strength data were collected during a trawl survey of hoki on the Chatham Rise in January 1999 and during an acoustic survey of hoki in Cook Strait in July/August 1999. A least squares method was used to estimate length to target strength relationships for hoki using a series of target strength distributions and associated trawls. New casts of hoki swimbladders were also used to generate target strength estimates.

Two target strength/fish length relationships were calculated using 1) a new least squares method with *in situ* data and 2) the new swimbladder modelling results. These are respectively:

$$TS = 75.2 \log_{10}(TL) - 177.6 \text{ and}$$

$$TS = 32.6 \log_{10}(TL) - 95.9$$

where TS is the target strength in dB re $1\mu\text{Pa}$ at 1 m, and TL the total length of the hoki in cm. The slope of the regression to the swimbladder data is significantly different to the *in situ* regression; possibly due to the neutral buoyancy assumption made when injecting the hoki swimbladders.

8. Objective

This report covers work arising from Objective 2 of Project HOK9803: "To refine estimates of target strength of hoki".

9. Methods

9.1 Introduction

The data analysed in this report were collected from the *Tangaroa* during a trawl survey of hoki on the Chatham Rise (January 1999) and from the *Kaharoa* during an acoustic survey of hoki in Cook Strait (July/August 1999). The data consist of *in situ* target strength (TS) data collected on specific acoustic marks, and casts of hoki swimbladders taken from freshly caught hoki. The *in situ* data were analysed using a new least squares method that estimates the length to target strength relationship using a series of TS distributions and fish length distributions from associated trawls. The swimbladder data were analysed using the mapping method (McClatchie *et al.*, 1996b).

9.2 Acoustic equipment description

Acoustic TS data were collected using a towed split-beam 38 kHz transducer. All of the data were processed and stored using the NIWA *CREST* data acquisition system (Coombs, 1994). The particular *CREST* system configuration was a four channel towed system, with underwater electronics, connected to a Simrad type ES38DD split beam transducer. The equipment and operational parameters used for the target strength data collection are given in Table 1.

CREST is computer based, using the concept of a 'software echo sounder'. It supports multi-channels, each channel consisting of at least a receiver and usually also a transmitter. The receiver has a broadband, wide dynamic range pre-amplifier and serial analog-to-digital converters (ADCs) which feed a digital signal processor (DSP56002). The ADCs have a conversion rate of 100 kHz and the data from these are complex (quadrature) demodulated, filtered and decimated. The filter was a 100 tap, linear-phase finite impulse response digital filter. For TS work the bandwidth was 4.86 kHz and the decimated frequency 10 kHz. Following decimation a 40 log R time-varied gain was applied. The results were shifted to give 16 bit resolution in both the real and imaginary terms and the complex data were stored for later processing.

The transmitter is a switching type with a nominal power output of 2 kW rms. It will operate over a wide range of frequencies (12–200 kHz). For TS work the transmitted pulse length was 0.32 ms (12 cycles at 38 kHz). Time between transmits was 1.4 seconds for data collected in Cook Strait, and 4 seconds for data collected on the Chatham Rise.

The receiver and transmitter were mounted in a flat-nosed, torpedo-shaped, 3 m long 'heavy weight' towed body.

The digital data from the receiver are sent to a control computer where they are combined with position and transect information and stored. The data are transmitted via the tow cable to the control computer on the towing vessel. All four transducer quadrants (beams) are energised simultaneously from a single transmitter but on receive, the system operates as four semi-independent echosounders. Data are processed independently on the four channels but operation is tightly synchronised by the transmit key and by using a common clock for all the ADCs. For TS the beams are

treated separately to reject multiple echoes and calculate the position of the echoes in the beam.

The acoustic systems were calibrated with the standard procedure (MacLennan & Simmonds, 1992) using a $38.1 \text{ mm} \pm 2.5 \text{ } \mu\text{m}$ diameter tungsten carbide sphere with a nominal TS of -42.4dB . Two nominally identical towed *CREST* systems were used and were calibrated in the deep tank at the NIWA Greta Point laboratories in December 1998, June 1999 and September 1999. They were also calibrated at sea (at depths ranging from 50 to 800 m) during October 1998, June 1999 and September 1999. All calibrations gave consistent results for each system. The resulting data from the various deep calibrations was fitted with two linear regressions:

$$\begin{aligned} S_{L1} &= 1.3 \cdot 10^3 \cdot d_{L1} + 60.5, \\ S_{H1} &= 5.8 \cdot 10^4 \cdot d_{H1} + 62.0, \end{aligned}$$

$$\begin{aligned} S_{L2} &= 1.6 \cdot 10^3 \cdot d_{L2} + 61.0, \\ S_{H2} &= 4.8 \cdot 10^4 \cdot d_{H2} + 62.0, \end{aligned}$$

where S_{Li} and S_{Hi} is the combined source level and transducer receiving response ($SL+SRT$) in dB re 1 V, and d_{Li} and d_{Hi} are the transducer depth in metres, i indicates the system number and $0 \leq d_{L1} \leq 440$, $d_{H1} > 440$, $0 \leq d_{L2} \leq 600$ and $d_{H2} > 600$. System 1 was used from the *Tangaroa* on the Chatham Rise and system 2 was used from the *Kaharoa* in Cook Strait.

9.3 Trawl data collection

Trawling was carried out using both bottom and midwater trawls. Trawls carried out from the *Tangaroa* used the standard NIWA 8 seam hoki bottom trawl with a 59 m groundrope, 45 m headrope and a cod-end mesh size of 60 mm (net plans contained in Hurst *et al.*, 1994). Rigging included 100 m long sweeps, 50 m bridles and 12 m backstrops. Midwater trawling from the *Tangaroa* was carried out using the NIWA Ymuiden P/159A midwater trawl with 150 m bridles and a 60 mm cod-end. Both gear types used 6.1 m^2 Super V trawl doors. All trawls from the *Kaharoa* used a midwater Resolution 4 panel net from Motueka Nets, with a 57 m groundrope, a 67 m headrope and a cod-end mesh of 70 mm. Rigging included 100 m bridles and used 2.85 m^2 high aspect cambered V doors. In operation the doorspread was approximately 84 m and the headline height 14 m (net plans are given in Stevenson (1997), with the only difference being that the cod end is now knotted).

All trawls were targeted on specific marks and were nominally 3 n. miles in length.

All catches were weighed, with more detailed biological information taken from hoki, ling and miscellaneous other species using the NIWA computerised wet-lab system.

Gonad stage data were not collected from the hoki caught in Cook Strait, but due to the time of the survey, and the fact that the hoki were caught in midwater it is assumed that they were spawning. Hoki caught on the Chatham Rise were not spawning.

9.4 *In situ* target strength data collection and processing

To collect *in situ* data, marks that were expected to be hoki were located and the towed transducer deployed 30–70 m above the marks, for several hours. The marks were then trawled to identify the species and to obtain an estimate of the size composition.

The recorded acoustic data preserve both amplitude and phase information and allows both target position and amplitude to be calculated. To estimate TS it is first necessary to filter out all echoes that do not originate from a single fish. To achieve this the following echo characteristics were checked:

- width of the combined beam
- relative width of the four beams
- phase stability of the combined beam
- phase stability of the individual beams
- proximity of other echoes
- similarity of amplitude between beams
- angle of arrival of the echo

These characteristics are based on those listed by Soule *et.al* (1995) and Soule *et.al.* (1997) and from discussions with Soule. They were used to filter data to reject all echoes formed by more than one fish. The values of these characteristics that were considered indicative of echoes from single fish were set by conducting an experiment involving two spheres at constant angles in the acoustic beam, but at a range of different distances (after Soule *et al.*, 1997). Echoes were considered to be from a single fish if the following conditions were met:

- The width of the echo was between 58% and 135% of the transmit pulse width at half the maximum echo amplitude (the 6dB amplitude points).
- The standard deviation of the electrical echo phase between the 6dB amplitude points was less than 0.2 radians on both the combined and individual echoes.
- The width of the four individual echoes at the 6dB amplitude points varied by less than 31% of the transmit pulse width.
- The echo peak was more than 0.75 m in range from other echoes.
- The mean and standard deviation of the difference between the echo amplitude on beam 1 and the same echo on beams 2, 3 and 4 was less than 1.5 and 3.0 dB respectively for all three comparisons.
- The estimated angle of arrival of the echo was within 3.55 degrees of the normal to the transducer face.

After filtering, the positions of the echoes remaining in the beam were calculated (Ehrenberg, 1979) and the amplitudes corrected accordingly. In addition, the maximum amplitude in each echo was estimated by fitting a quadratic to the three samples that made up the peak of the echo, and taking the maximum of this quadratic as the TS value for the subsequent data analysis.

9.5 The target strength estimation procedure

The estimation procedure assumes that there are one or more TS distributions available, and that for each TS distribution there are associated length frequencies for

one or more species. There are three main steps in the procedure: the determination of the TS modes; the determination of the length frequency modes; and the minimisation of a sum of squared residuals. In the sum of squares the observed values are the TS and length frequency modes, and the predicted values are those obtained from a simple model whose unknown parameters are the true length frequency modes and the coefficients of the length to TS relationships of all species present in the length frequencies.

Assume that there are n TS distributions and denote the j th mode in the i th TS distribution as T_{ij} and let m_i be the number of TS modes in the i th distribution. Further, let L_{isk} denote the k th mode for species s in the i th length frequency, and let m_{is} be the number of length frequency modes for species s in the i th length frequency. Note that some of the m_{is} may be equal to zero for some species.

The model assumes for each species a log linear relationship between TS and length:

$$TS_s(l) = a_s + b_s \log_{10}(l)$$

and that the true length modes l_{isk} may differ from the observed length modes:

$$l_{isk} = L_{isk} + \alpha_{isk}$$

where α_{isk} is an unknown error.

The independent unknown parameters in the model are therefore the a_s , the b_s , and the l_{isk} . They are estimated by minimizing the following sum of squares:

$$\sum_{isk} u_{isk} [l_{isk} - L_{isk}]^2 + w_{isk} [TS_s(l_{isk}) - TS_{isk}]^2$$

where the u_{isk} and w_{isk} are specified weights and TS_{isk} is the T_{ij} which is closest to $TS_s(l_{isk})$ in terms of minimum absolute difference. The rationale behind this approach is the hope that each length frequency mode will contribute to a mode in the corresponding TS distribution which on average is not too far away from the modal TS corresponding to the length frequency mode. Because the assignment of TS modes to length frequency modes is done simultaneously with the estimation of the length to TS parameters, the consistency of the assignments is guaranteed to the extent that the data are consistent (with the assumed model).

The use of weights in the sum of squares is to allow for different levels of sampling effort, or other measures of “quality” with regard to the data used in the TS distributions and length frequencies. In general, the better the “quality” of a distribution the higher the weight it should be given. With regard to the length frequencies, the higher the weight assigned to a mode the closer the predicted mode will be to the observed mode.

Further details on the estimation procedure is given in Cordue *et al.* (Cordue *et al.*, *in prep.*).

9.6 Application of estimation procedure to the acoustic data set

On each of the voyages, there were some occasions on which more than one trawl sampled the layer from which target strength data were collected. In the fitting procedure, each trawl was used separately; that is the target strength distribution was paired with each of the corresponding trawls in turn.

The modes in the target strength distributions (Figure 1) and the length frequencies (Figure 2) were determined algorithmically, as detailed in Cordue *et al.* (Cordue *et al.*, *in prep.*).

The specified weights for the sum of squares were calculated as the product of a (trawl) station weight and a constant “length frequency weight” (for the length mode portion of the sum of squares) or the station weight and a constant “target strength weight” (for the target strength portion of the sum of squares). The “length frequency weight” was 0.5 and the “target strength weight” was 1. The station weights were either 0.1 (when the hoki catch was less than 100 kg, and the hoki length frequency was used on that station), 2.0 for length frequency sample sizes from 500 to 700, or 1.0 for sample sizes up to 400 (see Table 3). In an alternative weighting scheme the weights of 0.1 were replaced by weights of 1.

The baseline estimation used the “main modes” with the weighting scheme which down-weighted stations with low hoki catch. Two sensitivity runs were also done. Both used the alternative simpler weighting scheme, one with the “main modes”, and the other using the larger set of length frequency modes.

In each of the three estimation runs, the slope of the hoki target strength relationship was estimated within the interval [5, 95]. This interval was partitioned into nine or ten sub-intervals and each sub-interval was used to bound the hoki slope while an estimation was done using 300 random starting values for the minimizer. This procedure was done for two or three further narrow sub-intervals (including a forced hoki slope of 20) so that the general trend in the sum of squares surface was determined for each run. In the baseline run, a further estimation was done using bounds on the hoki slope which included the best estimate from the initial runs. In this final estimation, 5000 random starting values were used and the global minimum was determined. The bootstrap procedure was only applied to the baseline estimation results and 1000 simulations were used to determine a 99% confidence region for the hoki regression line.

9.7 Swimbladder modelling

Casts were made of hoki swimbladders by injecting freshly caught hoki with epoxy resin. The volume of resin used was 3.1% of the whole fish volume. This is the level estimated to be required for neutral buoyancy (Grimes *et al.*, 1997).

A selection of these casts covering the whole size range were analysed as follows:

- Each cast was embedded in a block of resin then sectioned at measured intervals of either 0.25, 0.5, or 1 cm,
- The section perimeters were digitised to construct a 3D model of each cast,
- The TS for each cast was calculated using the mapping method of McClatchie *et al.* (1996b) at 38 kHz with a fish tilt angle distribution of 0° and standard

deviation 15° , and also at tilt angle distributions of -11.8° , 0° , and 11.8° with standard deviations of 29° and 15° (corresponding to *in situ* measurements of hoki tilt angle using stereo underwater cameras; see Coombs and Cordue (1995)).

A 3D model was generated from the digitised swimbladder casts and used as a visual check that the process of constructing the 3D model had worked correctly.

Casts were made of 23 fully inflated hoki swimbladders, of which ten were processed to estimate tilt averaged target strength at 38 kHz. The ten casts covered fish sizes from 26 to 95 cm total length.

Intact undamaged hoki swimbladders are rare in trawl caught fish (less than 5%). As well as this the success rate in injecting intact swimbladders to the correct level without major leakage is less than 30%. Hence obtaining a selection from all size groups is difficult – especially so for the less frequent length groups.

To overcome this problem the 3D models of each successful cast were scaled using new data on changes in swimbladder length and width with fish length. This resulted in a series of target strength points against fish length for each cast. Data on swimbladder length and width were collected from 53 hoki from 25 to 105 cm in length by measuring the length and width of the “footprint” left by the swimbladder where it is attached to the roof of the abdominal cavity. The regression equations for fish length against swimbladder length and swimbladder width were effectively linear for these 53 fish. This regression was used to scale the 3D models of each of the casts. The scaled casts were then used to produce a series of TS estimates at increments of 5 cm for lengths between 20 and 120 cm. The hoki injected with resin had cast and imprint measurements recorded. From the comparison of both sets of data a correction factor was obtained and applied to the imprint measurements.

10. Results

10.1 Trawling results

Nineteen trawls were carried out in support of the target strength data (Table 2). A summary of the catch from these trawls is given in Table 3.

Hoki was the primary catch for most of the trawl stations with most catches of hoki being greater than 200 kg and making up 70% or more of the total catch by weight (Table 3). Hoki catches of less than 100 kg were made on four of the stations. For the small hoki catches, all of the hoki were measured. When larger catches were made, sub samples were taken with typically between 250 and 700 hoki being measured (Table 3).

In total, the largest bycatch over the trawl stations came from spiny dogfish, with sea perch making the next largest contribution (Table 3). On the *Tangaroa* trawl stations a bottom trawl was used and much of the bycatch came from what are probably bottom-dwelling species which would therefore make little contribution to the acoustic backscatter. Sea perch, lookdown dory, and ghost shark would fall within this category. For the bycatch species the length frequency sample sizes were typically less than 100 and there were no common species between the *Kaharoa* and *Tangaroa* voyages (Table 4).

10.2 *In situ* results

A total of about 30 hours of target strength data was collected during the two voyages. There were three target strength sets on the *Kaharoa* voyage (KAH9911) and seven on the *Tangaroa* voyage (TAN9901). The *Kaharoa* target strength sets were very successful in the number of detected single echoes, with between about 80 000 and 380 000 targets being accepted in each of the three sets (Table 5).

Two examples of the hoki length frequencies and associated target strength distributions used in the analysis are given in Figure 3. In the baseline analysis only the main modes were used (e.g., for station 9 the possible mode at 30 cm was used in a sensitivity run but excluded from the baseline run (Figure 3a)). A small length frequency sample size does not necessarily mean that the length modes are not well defined. Arguably, the single mode for station 131 is better defined than the two modes for station 9 (Figure 3a & c) despite the lower sample size (*see* Table 3). The second *Kaharoa* TS set has a very smooth distribution when a step size of 1 dB is used (Figure 3b). This is due to its enormous sample size (381 000). In comparison, the sixth *Tangaroa* set with a moderate sample size (21 000) is only relatively smooth when a step size of 2 dB is used (Figure 3d).

In the baseline run and the two sensitivity runs the global minimum for the sum of squares occurred when the slope of the hoki length to TS relationship was 5, being the lowest value of the range considered (Figure 4). Such a low value is implausible and it should be noted that a slope of 0 would yield an even better fit. In each of the three runs there was a general dip in the sum of squares when the hoki slope was near to 75. However, for slopes of about 20, a better fit can be achieved in each of the three runs than is possible for slopes of about 75 (Figure 4).

When the minimisation was done in each of the three runs, while restricting the hoki slope to between 65 and 85, the best fits were obtained at hoki slopes from 73.3 to 77.5 (Table 6).

In the baseline case (with the estimated slope at about 75) the fit to the associated pairs of length and TS modes appears reasonable (Figure 5). The relationship is also consistent with three previously estimated *in situ* points (Figure 5). The previously estimated hoki TS relationships of “Macaulay” (Macaulay & Grimes, 2000) and Bradford (1999) are on the edge of the estimated confidence region (Figure 6). The estimate of “Grimes” from the latest swimbladder modelling results (§10.3), which has a neutral buoyancy assumption, is clearly inconsistent with the modal estimate (Figure 6).

When a hoki slope of 20 is imposed on the minimisation, the resultant fit is also reasonable, except that the predicted values for lengths above 70 cm are all higher than the observed values (Figure 7). However, this relationship is not consistent with the previous *in situ* points (Figure 7) or with any of the other estimated relationships (Figure 8).

10.3 Swimbladder modelling results

The swimbladder modelling results for a tilt distribution with a mean of 0° and standard deviation of 15° are presented in Table 7. The mean tilt angle averaged target strength for the other means and standard deviations mentioned in §9.7 resulted in

minor changes to the target strength estimates. The results from the scaled swimbladders are given in Figure 11. The scaled results exhibit dips in the target strength value at various swimbladder lengths. The tilt-averaged target strength is obtained by convolving the modelled TS/tilt angle response with a tilt distribution (normal with a mean of 0° and a standard deviation of 15°). This serves to complicate any explanation of the behaviour of the TS/FL curves. By considering the TS/tilt relationship separately, a greater understanding of the behaviour of the TS/FL relationship can be obtained.

The TS/tilt relationship is characterised by a series of peaks and nulls (Figure 9). These nulls are a result of destructive interference of the scattered acoustic wave from different parts of the swimbladder. As the tilt angle changes, the 'line-of-sight' distance between various parts of the swimbladder changes, and hence the amount of constructive and destructive interference changes. As the size of the swimbladder varies, the position, number and intensity of these nulls vary. When nulls move into the tilt angle range that is used in the convolution they reduce the tilt-averaged target strength. As the fish size increases, the number of nulls increases and produces more dips in the TS/FL curve. Figure 10 contains target strength data for a range of swimbladder sizes and tilt angles and is effectively a composite of many Figure 9's. The movement of the nulls into the region that is used in the convolution (between the two horizontal lines) can be seen clearly. The tilt averaged target strength is displayed for comparison.

It is expected that for a real fish the various contributions to the scattering from other parts of the fish (bones, flesh, etc) will reduce the severity of the nulls and produce a smoother TS/tilt curve and hence a smoother TS/FL curve.

10.4 Discussion

10.4.1 Estimation method

For any estimation method it is important to understand the strengths and limitations of the method in terms of the reliability of the estimates that it provides. The method used in this report assumes that there is a one to one correspondence between length frequency modes and TS modes for each species for which a length to target strength relationship is estimated. It is known that for some species that such a relationship does not necessarily hold. On occasion, a single species layer with a uni-modal length frequency has been seen to produce a bimodal TS distribution and it has been shown that such an occurrence can be predicted from swimbladder modelling results (Williamson & Traynor, 1984). The method proposed in this report will not work well with such species. However, the same type of modelling approach can still be used.

The estimation method used in this report is fairly robust to TS modes caused by species not used in the estimation procedure. Provided that the model assumptions are satisfied and there isn't too much observation error, the method allows any number of spurious TS modes to be ignored in favour of those modes which yield the best fit. If there is too much observation error then TS modes may not be assigned to the correct species. However, if the data set includes stations from single species layers with a uni-modal length frequency, then the estimation of the length to TS relationship for these species will be much more robust, especially so if such layers cover a large length range.

The proposed boot-strapping procedure provides a useful indication of the confidence that can be placed in the estimates for a given species. However, it underestimates the level of uncertainty in the relationship because it does not allow for alternative correspondences between length and TS modes. A better method would be to bootstrap the full estimation procedure, but this is somewhat problematic because an allowance would need to be made for all of the species which contributed to the TS modes (i.e., not just those species which are represented in the length frequencies). One possibility would be to attribute TS modes which were not assigned to the represented species, to the minimum number of unknown species which would explain them.

10.4.2 Hoki data set

The use of the least squares method on the hoki data set is probably acceptable in regard to the issue of whether there is a one to one correspondence between hoki length modes and hoki TS modes. The early swimbladder modelling results of Grimes *et al.* (1997) were used to create simulated TS distributions for uni-modal length frequencies with a range of tilt angle distributions. All of the simulated TS distributions were uni-modal because there was sufficient variation in the TS response at angle for fish of the same length. In simulations which did not include variation in response at angle for a given fish length, it was easy to generate a bimodal TS distribution from a uni-modal length frequency, provided that the tilt angle distribution extended beyond the occurrence of the first nulls (or very low TS values) and that the TS response at angle was symmetric about the mode of the tilt angle distribution.

The variance in individual modal TS distributions was examined visually for each TS mode that was associated with a hoki length mode (in the baseline run). The standard deviations ranged from about 3 to 5 dB. Given that this variation is due to variation in length, possible multiple species composition, sampling variance, and the *tilt angle* distribution, it was considered that there would be little error in using modal TS as a proxy for tilt averaged TS.

The estimated slope of about 75 for the hoki TS relationship seems dubious given estimates of slopes for other fish species and the rather common practice of assuming a slope of 20 (Foote, 1979). McClatchie *et al.* (1996a) provide a range of estimates for regressions of maximum dorsal aspect TS using a large collection of published data. Their slope estimates range from about 10 to 25, and the 95% confidence intervals for the slopes of any of the species do not extend beyond 30. They do note that hoki is atypical of gadoids having a small swimbladder relative to its length because of a long tapering tail. This explains why it may have a lower TS at length than a typical gadoid, but does not suggest that the slope of the length to TS relationship would be steeper than that of other gadoids.

When a slope of 20 was imposed in the modal fitting for the hoki data set, the fit was better than at a slope of 75. However, the regression line was inconsistent with the early *in situ* data points accepted by Bradford (1999), the early swimbladder modelling results (Grimes *et al.*, 1997) and the regression line from modal association by eye (Macaulay & Grimes, 2000) (*see* Figure 7 and Figure 8). In contrast, the regression with the slope at 75 was consistent with these results (*see* Figure 5 and Figure 6). The swimbladder modelling results presented in this report (§10.3) made a neutral buoyancy assumption to determine how much to inflate the swimbladders. The

higher intercept and the flatter slope of this relationship compared to the other estimated relationships (*see* Figure 6) suggest that the neutral buoyancy assumption is incorrect, and that smaller hoki maintain a higher magnitude of negative buoyancy than larger hoki.

It is possible that the estimated slope of about 75 is correct. Part, but not all, of the steep slope can be explained by the relative growth rates of the swimbladder and the fish length (the early swimbladder modelling results gave an estimated slope of about 55). The additional steepness could be explained by a trend in tilt angle distribution with length. Smaller hoki are more vulnerable to predators than larger hoki and therefore could be expected to maintain a greater level of negative buoyancy to enable a quicker dive response when threatened. However, this is somewhat speculative and more data will be required before hoki TS can be estimated with confidence.

11. Conclusions

A least squares method for estimating the target strength to fish length relationship has been developed and used to estimate a relationship for hoki using new *in situ* data. This relationship is:

$$TS = 75.2 \log_{10} TL - 177.6,$$

where TL is hoki total length in cm, and TS is the target strength in dB re $1\mu\text{Pa}$ at 1 m.

Ten new swimbladder target strength points have been calculated, covering a hoki length range of 26 to 95 cm. The new technique of scaling the swimbladder casts has been used to provide a large number of target strength/fish length points, and a regression fitted to these points is:

$$TS = 32.6 \log_{10}(FL) - 95.9,$$

where TL is hoki total length, and TS is the target strength.

12. Publications

A request has been made to the Ministry of Fisheries to submit Cordue *et al.* (*in prep.*) to the Journal of the Acoustical Society of America.

13. Data storage

Data collected from trawling is stored in the New Zealand Ministry of Fisheries Trawl survey database. Acoustic data is stored in the Ministry of Fisheries Acoustics Database.

14. Acknowledgements

We thank Ian Doonan, Sam McClatchie, and other members of NIWA's acoustic group for useful discussions on this work.

15. References

- Bradford, E., 1999. Acoustic target strength of hoki. *Final Research Report for Ministry of Fisheries Research Project HOK9703, Objective 2*, NIWA.
- Coombs, R., 1994. An adaptable acoustic data acquisition system for fish stock assessment, International Conference on Underwater Acoustics, Australian Acoustical Society, Australia.
- Coombs, R.F. & Cordue, P.L., 1995. Evolution of a stock assessment tool: acoustic surveys of spawning hoki (*Macruronus novaezelandiae*) off the west coast of South Island, New Zealand, 1985–91. *New Zealand Journal of Marine and Freshwater Research*, 29: 175–194.
- Cordue, P.L., Coombs, R.F. & Macaulay, G.J., *in prep.* A least squares method of estimating length to target strength relationships from *in situ* target strength distributions and length frequencies.
- Ehrenberg, J.E., 1979. A comparative analysis of *in situ* methods for directly measuring the acoustic target strength of individual fish. *IEEE Journal of Oceanic Engineering*, OE-4(4).
- Foote, H.G., 1979. On Representing the Length Dependence of Acoustic Target Strengths of Fish. *J. Fish. Res. Board. Can.*, 36: 1490–1496.
- Grimes, P., McClatchie, S. & Richards, L., 1997. A re-calculation of target strength from hoki swimbladder casts using original data from Do and Surti (1990) and Coombs and Cordue (1995). *Client report to the New Zealand Ministry of Fisheries*.
- Hurst, R.J. & Bagley, N.W., 1994. Trawl survey of middle depth and inshore bottom species off Southland, February–March 1993 (TAN9301). *New Zealand Fisheries Data Report*, 52, 58 pp.
- Macaulay, G. & Grimes, P., 2000. Estimation of acoustic target strength of hoki using *in situ* and swimbladder modelling. *New Zealand Ministry of Fisheries Research Progress Report*.
- MacLennan, D.N. & Simmonds, E.J., 1992. *Fisheries Acoustics*. Fish and Fisheries Series; 5. Chapman & Hall, London, 325 pp.
- McClatchie, S., Aslop, J. & Coombs, R.F., 1996a. A re-evaluation of relationships between fish size, acoustic frequency, and target strength. *ICES Journal of Marine Science*, 53: 780–791.
- McClatchie, S., Aslop, J., Ye, Z. & Coombs, R.F., 1996b. Consequence of swimbladder model choice and fish orientation to target strength of three New Zealand fish species. *ICES Journal of Marine Science*, 53: 847–862.
- Soule, M., Barange, M. & Hampton, I., 1995. Evidence of bias in estimates of target strength obtained with a split-beam echosounder. *ICES Journal of Marine Science*, 52: 139–144.

- Soule, M., Barange, M., Solli, H. & Hampton, I., 1997. Performance of a new phase algorithm for discriminating single and overlapping echoes in a split-beam echosounder. *ICES Journal of Marine Science*, 54: 934–938.
- Stevenson, M.L., 1997. Inshore trawl survey of the Canterbury Bight and Pegasus Bay December 1996–January 1997 (KAH9618). *NIWA technical report*, 7, NIWA, Wellington, 14 pp.
- Williamson, N.J. & Traynor, J.J., 1984. *In situ* target–strength estimation of Pacific whiting (*Merluccius productus*) using a dual–beam transducer. *Journal du Conseil Permanent International pour l'Exploration de la Mer*, 41: 285–292.

Table 1: Configuration of the echosounders used to collect target strength data

System number	1	2
Transducer model	Simrad ES38DD	Simrad ES38DD
Transducer serial no.	28326	28327
Nominal 3dB beamwidth(°)	6.9	7.0
Effective beam angle (sr)	0.0079	0.0079
Operating frequency (kHz)	38.156	38.156
Transmit interval (s)	4.0	1.4
Nominal pulse length (ms)	0.32	0.32
Filter bandwidth (kHz)	4.86	4.86
Initial sample rate (kHz)	100.0	100.0
Decimated sample rate (kHz)	10.0	10.0
TVG	40 log R + 2αR	40 log R + 2αR
Nominal absorption (dB/km)	8.0	8.0
SL+SRT (dB re 1 V at 1 m)	61.1	61.8
Calibration valid at (m)	400	400
20log10G	49.7	49.5

Table 2: Trawl station data for trawls associated with target strength transects for *Kaharoa* (7–13) and *Tangaroa* (117–142). Times are NZST for trawls 7–13 and NZDT for trawls 117–142

Trawl	Start date	Start time	Start latitude	Start longitude	Trawl type	Mean trawl depth (m)	Mean bottom depth (m)
7	3-Aug-99	0825	41.539 S	174.577 E	MW	312.5	490
8	8-Aug-99	1752	41.536 S	174.574 E	MW	303	470
9	9-Aug-99	0628	41.603 S	174.776 E	MW	429	605
10	9-Aug-99	0812	41.603 S	174.758 E	MW	405.5	630
11	9-Aug-99	1714	41.604 S	174.767 E	MW	368.5	575
12	10-Aug-99	0704	41.128 S	174.584 E	MW	278	295
13	10-Aug-99	1712	41.127 S	174.586 E	MW	275	297.5
117	22-Jan-99	1610	43.285 S	175.962 E	BT	376.5	376.5
118	22-Jan-99	1838	43.276 S	175.964 E	BT	372.5	372.5
119	23-Jan-99	0223	43.249 S	175.938 E	BT	380.5	380.5
120	23-Jan-99	0518	43.297 S	176.260 E	BT	337.5	337.0
121	23-Jan-99	0738	43.293 S	176.260 E	BT	338.0	337.5
122	23-Jan-99	1501	43.299 S	176.193 E	MW	320.5	317.0
130	24-Jan-99	1500	43.933 S	176.674 E	BT	488.5	488.5
131	25-Jan-99	0108	43.932 S	176.683 E	BT	497.5	497.5
132	25-Jan-99	0220	43.948 S	176.699 E	BT	504.0	504.0
133	25-Jan-99	0341	43.956 S	176.672 E	BT	504.0	504.0
141	26-Jan-99	0741	44.051 S	176.819 E	BT	588.5	588.5
142	26-Jan-99	0915	44.051 S	176.829 E	BT	593.5	593.5

Table 3: For each trawl station, the station weight used in the sum of squares, the catch of hoki, the percentage of hoki in the total catch (by weight), the number of hoki measured, and the catch of the main bycatch species. CBO: Bollen's rattail, COL: Oliver's rattail, GSH: ghost shark, LDO: lookdown dory, RBM: Ray's bream, SPD: spiny dogfish, SPE: sea perch

Trawl station	Station weight	Hoki catch (t)	Hoki catch /total catch (%)	No. of hoki measured	Bycatch species catch (when ≥ 80 kg.)
7	2	1.1	79	608	SPD 273
8	1	0.3	81	160	
9	1	0.4	99	257	
10	1	0.5	99	393	
11	1	0.4	97	260	
12	2	0.5	85	666	
13	2	0.4	85	586	
117	2	2.4	80	617	LDO 114, SPD 107, SPE 88
118	2	1.3	78	612	SPD 95
119	0.1	0.04	32	91	
120	2	4.2	91	679	GSH 147
121	2	2.3	76	626	SPD 175, SPE 243
122	2	0.4	82	516	RBM 88
130	2	1.2	70	629	CBO 168, COL 82
131	0.1	0.07	36	76	
132	0.1	0.09	32	103	
133	1	0.03	18	40	
141	1	0.2	49	254	
142	1	0.4	64	372	

Table 4: The length frequency sample size for each trawl station for the bycatch species used in the analysis. "--" indicates that less than 50 were measured for that station. FRO: frost fish, CBI: two-saddle rattail, JAV: javelin fish, COL: Oliver's rattail, CBO: Bollen's rattail

Species code	Station number									
	12	13	121	130	131	132	133	141	142	
FRO	53	53	-	-	-	-	-	-	-	
CBI	50	100	-	-	-	-	-	-	-	
JAV	-	-	119	122	60	82	79	112	100	
COL	-	-	-	103	86	135	97	69	-	
CBO	-	-	-	115	-	76	-	87	60	

Table 5: Date and amount of acoustic target strength data collected and associated tows

Voyage	Set	Date	Hours of data	No. of single echoes (000's)	Mean transducer depth (m)	Associated tows
KAH9911 (Cook Strait)	K1	3 Aug 1999	2.5	153	272	7, 8
	K2	9 Aug 1999	4.5	381	309	9, 10, 11
	K3	10 Aug 1999	5.1	88	233	12, 13
TAN9901 (Chatham Rise)	T1	22-23 Jan 1999	3.4	31	298	117, 118, 119
	T2	23 Jan 1999	3.1	31	247	120, 121, 122
	T3	24 Jan 1999	1.2	16	424	130
	T4	24 Jan 1999	1.2	12	423	133
	T5	24 Jan 1999	1.2	10	426	132
	T6	24-25 Jan 1999	2.5	21	360	131
	T7	26 Jan 1999	3.1	34	510	141, 142

Table 6: The estimated length to TS relationships for hoki in the baseline and sensitivity runs

	Intercept	Slope
Baseline	-177.6	75.2
Main modes	-174.8	73.3
All modes	-183.9	77.5

Table 7: Target strength estimates from swimbladder modelling. The modelling process is accurate to approximately 0.1 dB

Fish length (cm)	Cast number	<TS>
94.5	1	-32.0
74.1	2	-36.5
69.3	16	-39.5
31.0	17	-43.8
47.3	18	-45.8
41.1	19	-46.3
27.1	20	-47.1
28.5	21	-46.4
26.4	22	-47.7
28.0	23	-46.5

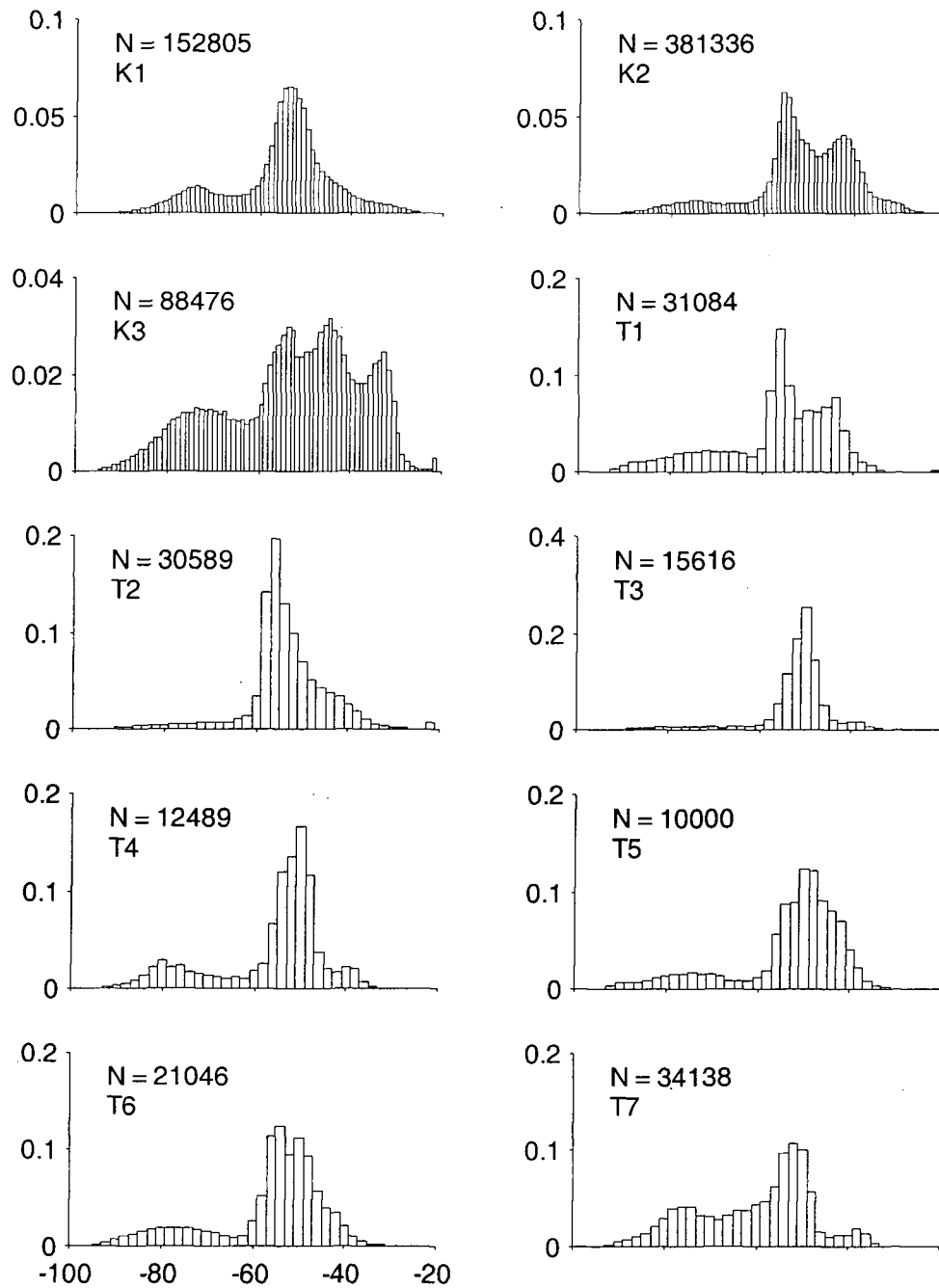


Figure 1: In situ target strength distributions from the *Kaharoa* (K labels) and the *Tangaroa* (T labels). All of the x-axes are the same.

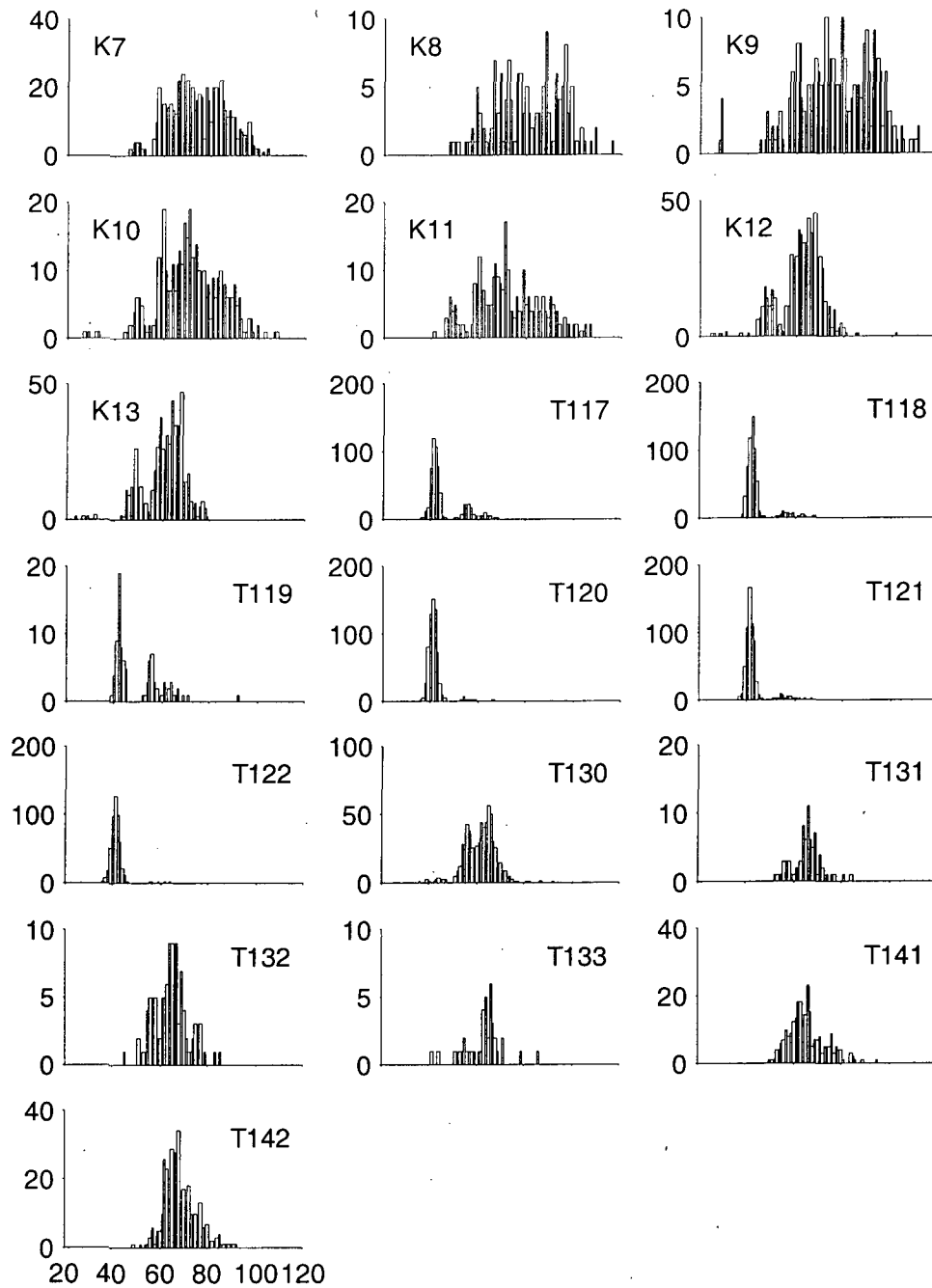


Figure 2: Hoki length distributions from the *Kaharoa* (K labels) and the *Tangaroa* (T labels). All of the x-axes are the same.

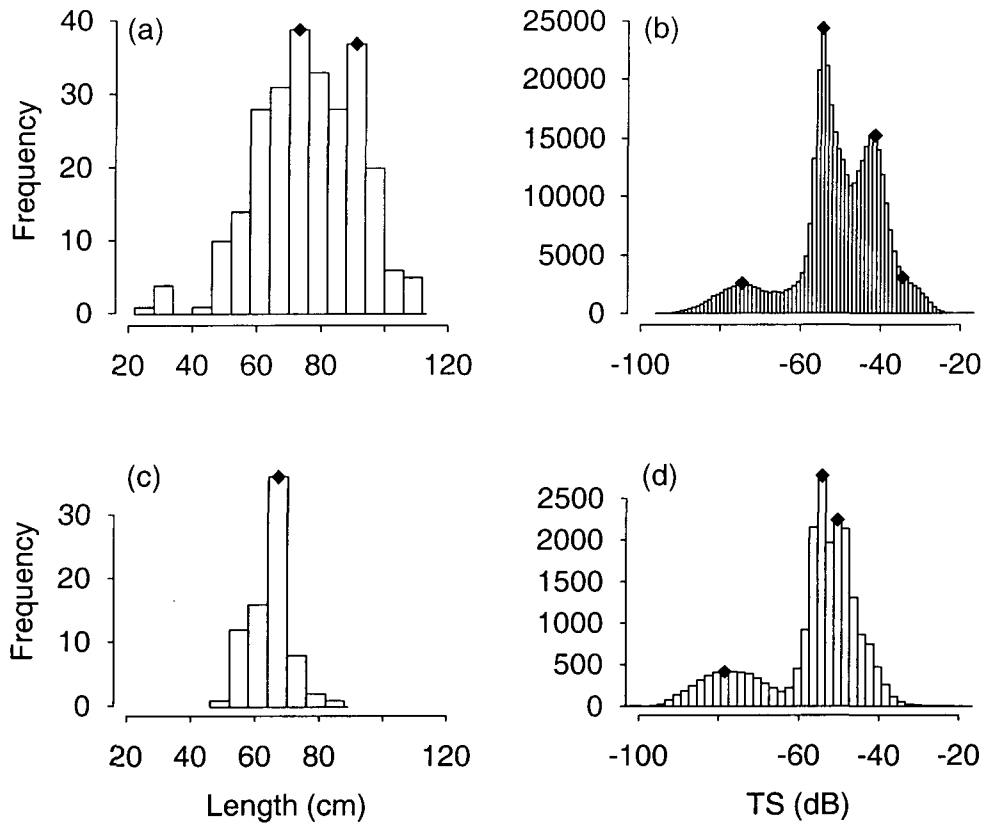


Figure 3: Examples of modes and a shoulder (see (b)) for hoki length frequencies and associated target strength distributions used in the estimation procedure: (a) hoki length frequency from the *Kaharua* voyage, station 9; (b) TS distribution after single target filtering for *Kaharua* set 2; (c) hoki length frequency from the *Tangarua* voyage, station 131; (d) TS distribution after single target filtering for *Tangarua* set 6.

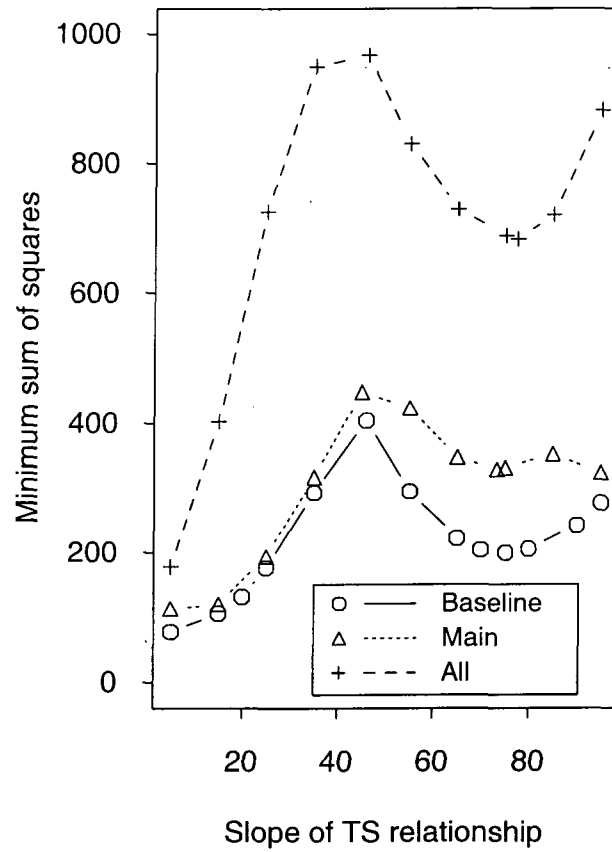


Figure 4: The general trend in the shapes of the sums of squares surfaces, with regard to the slope in the length to TS relationship for hoki, for the baseline run and the two sensitivity runs: “Main” uses the same length modes as the baseline but with a different weighting scheme. “All” uses the same weights as “Main” but with a much larger number of length modes.

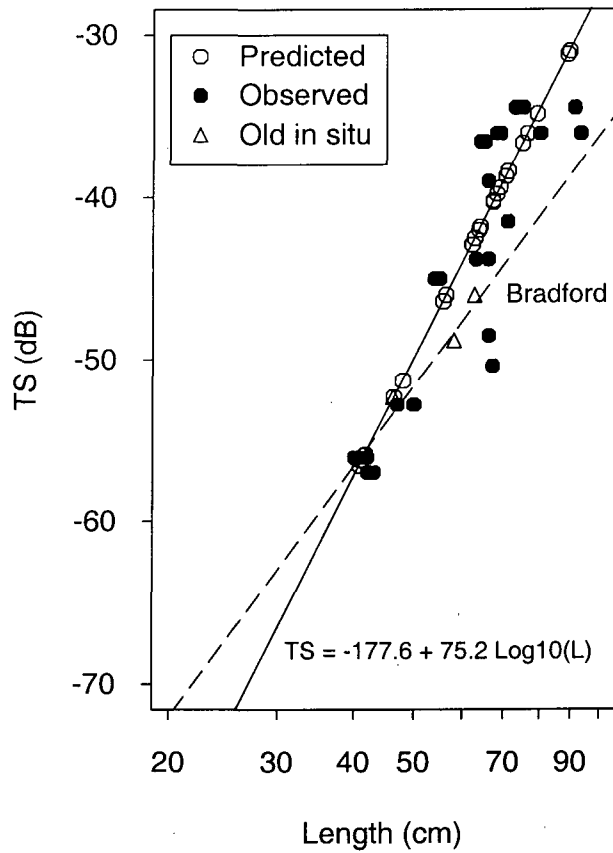


Figure 5: The fitted length to target strength relationship for hoki in the baseline case (solid line). The relationship for hoki derived by Bradford (1999) is also shown (dashed line) with the three previously accepted *in situ* data points (triangles).

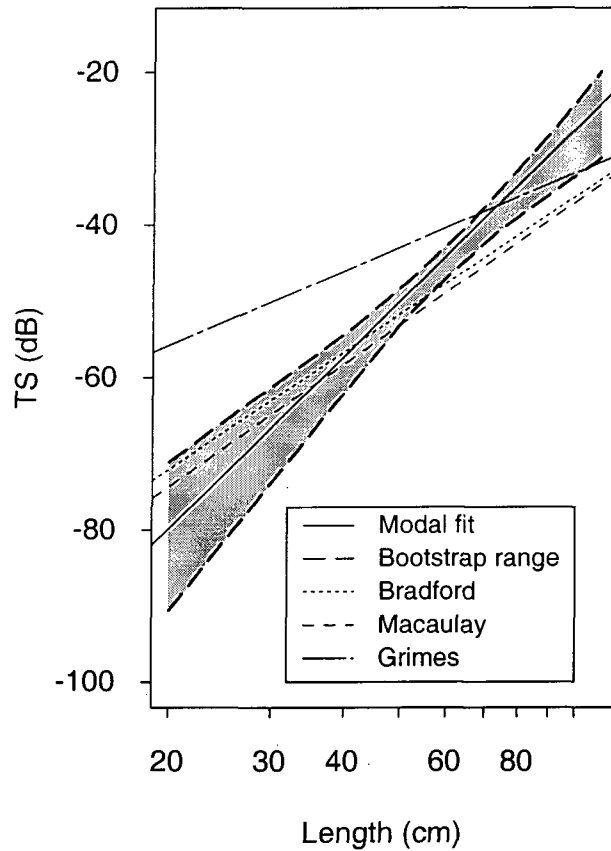


Figure 6: The fitted length to target strength relationship for hoki in the baseline case (solid line) with a 99% confidence region. The relationships for hoki derived by Bradford (1999), and Macaulay and Grimes (2000) are also shown. The “Macaulay” relationship used *in situ* data and the “Grimes” relationship was from swimbladder modelling which used a neutral buoyancy assumption.

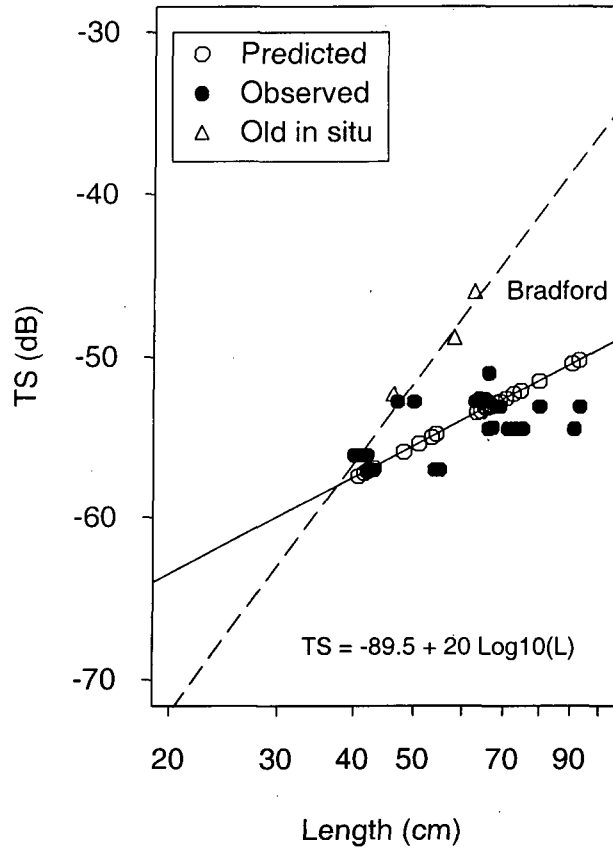


Figure 7: The fitted length to target strength relationship for hoki when a slope of 20 is assumed (solid line). The relationship for hoki derived by Bradford (1999) is also shown (dashed line) with the three previously accepted *in situ* data points (triangles).

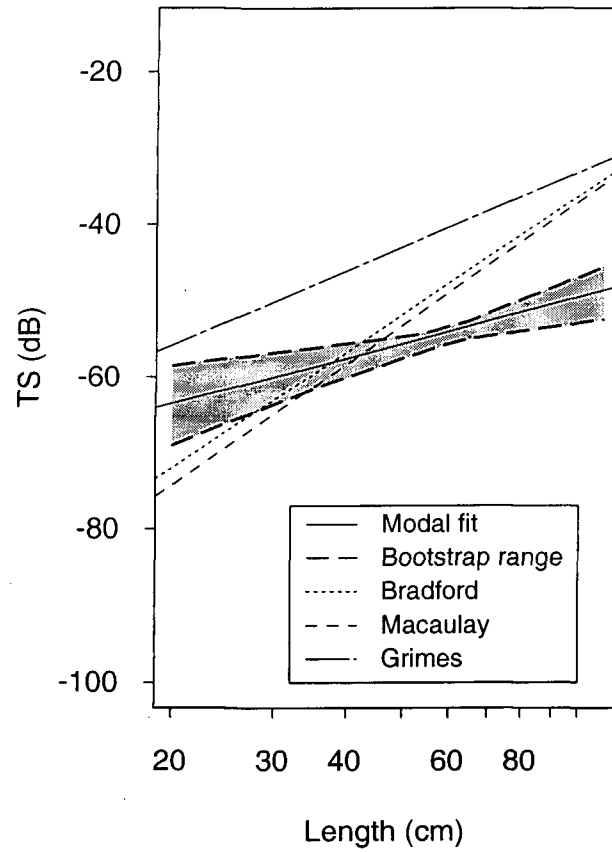


Figure 8: The fitted length to target strength relationship for hoki when a slope of 20 is assumed (solid line) with a 99% confidence region. The relationships for hoki derived by Bradford (1999), and Macaulay and Grimes (2000) are also shown. The “Macaulay” relationship used *in situ* data and the “Grimes” relationship was from swimbladder modelling which used a neutral buoyancy assumption.

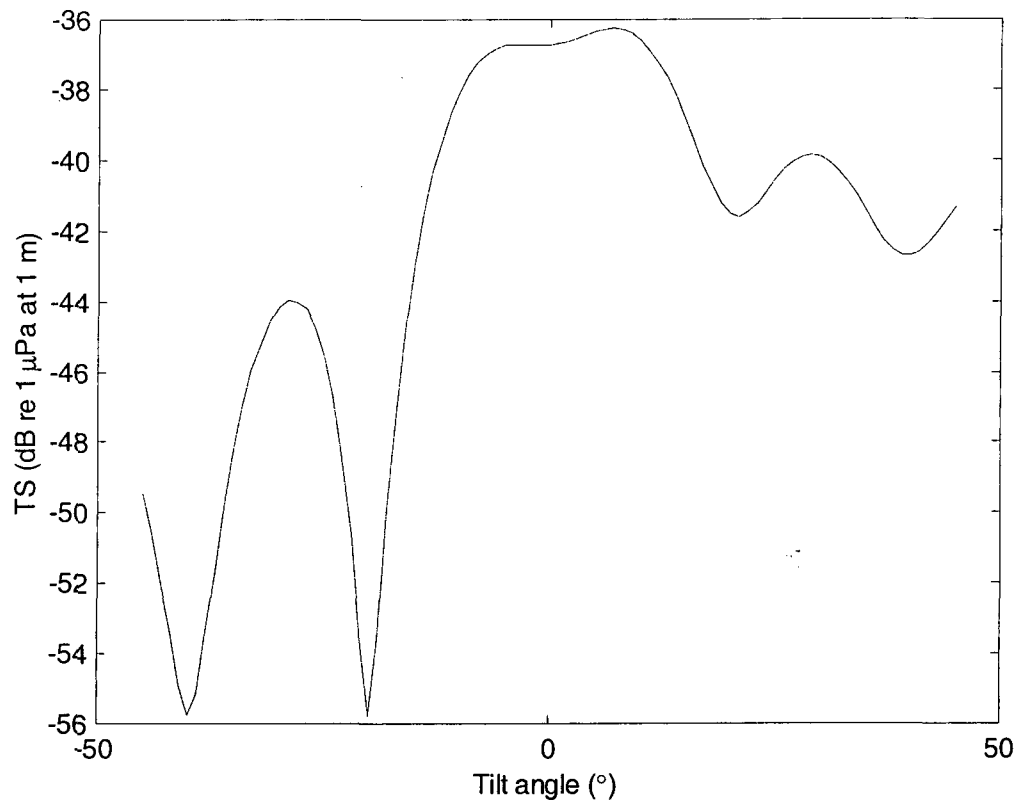


Figure 9: An example of the TS/tilt relationship obtained from swimbladder models of hoki.

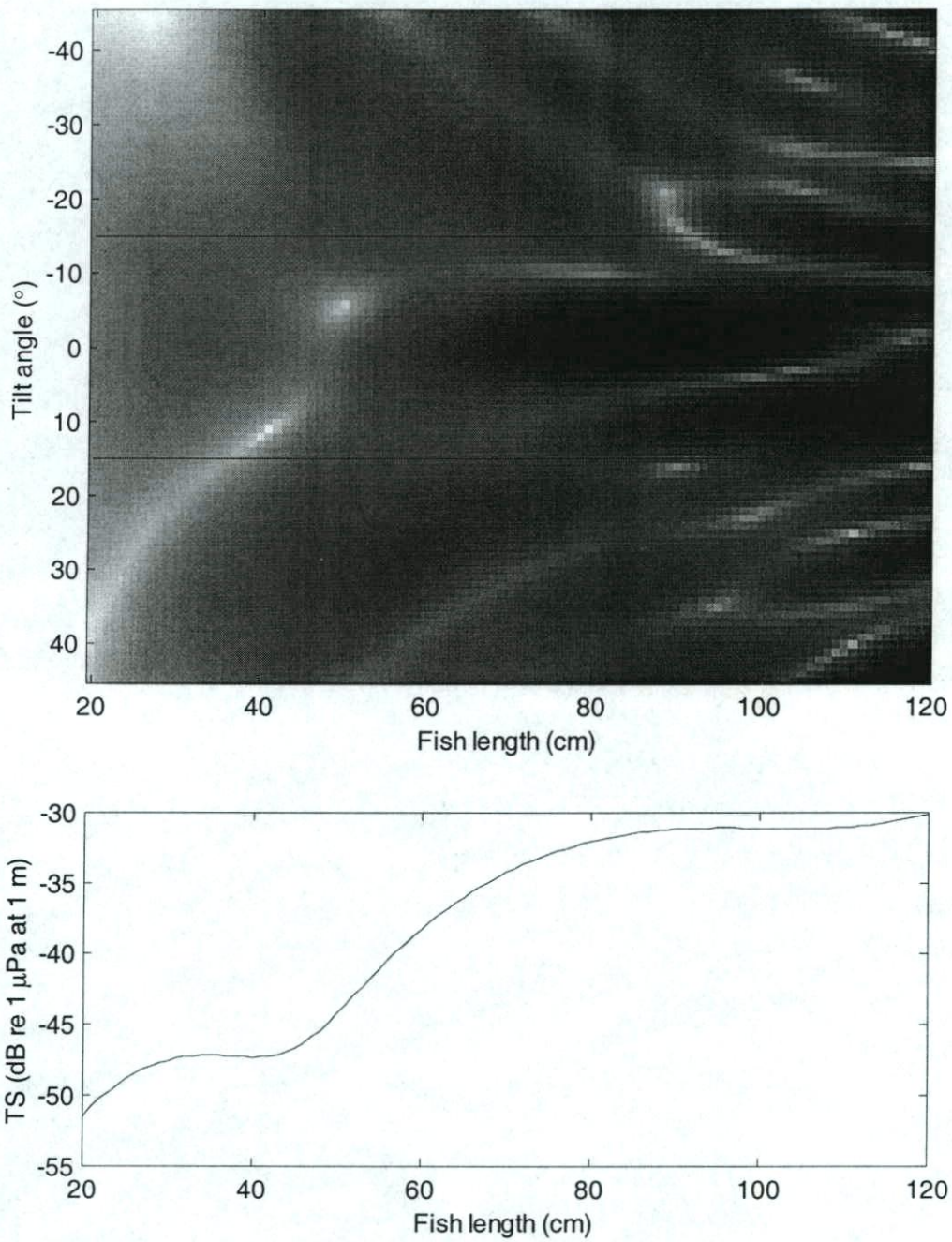


Figure 10: Hoki target strength at various fish lengths and tilt angles. Lighter shades indicate lower target strength values (upper figure). The corresponding tilt averaged target strength curve is given in the lower figure (using a normal distribution with a mean of 0° , and standard deviation of 15°).

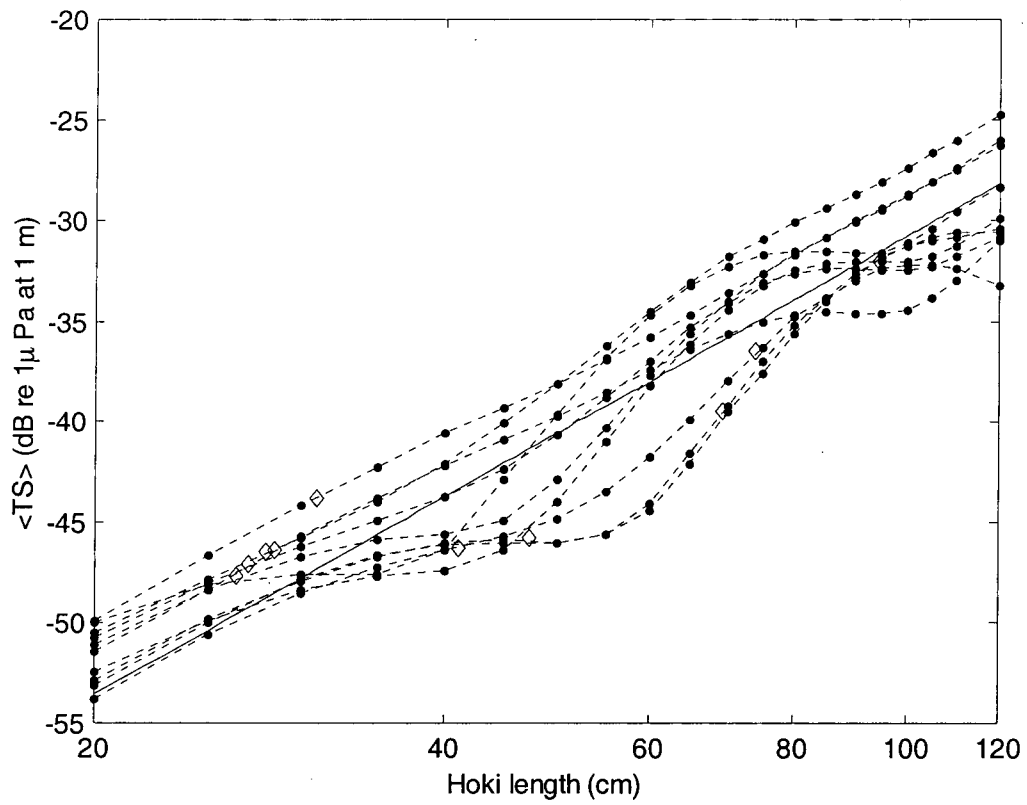


Figure 11: The results from the swimbladder modelling. The target strength of the actual swimbladders is given by the diamonds, and the scaled swimbladders by the dots. The straight line is a regression through the scaled swimbladder data.

